Axial load limit considerations for 14 in. square prestressed concrete piles

John C. Ryan and Timothy W. Mays

- This research analyzed the moment-curvature response of 14 in. (350 mm) square prestressed concrete piles for varying axial loads. The moment-curvature analysis was performed using structural analysis and design software.
- In previous research, axial load limits were recommended for 14 in. (350 mm) square prestressed concrete piles to prevent loss in moment relative to the first peak moment, which was believed to result in unreliable seismic performance; however, 14 in. piles have a second peak that can vary from 80% of the first peak to over 100% of the first peak moment in most cases.
- Results presented in this paper suggest that more-accurate load limits can be established. In addition, the use of an axial load limit to ensure acceptable seismic performance may not be reasonably justified.

PCI Journal (ISSN 0887-9672) V. 66, No. 6, November–December 2021.

PCI Journal is published bimonthly by the Precast/Prestressed Concrete Institute, 8770 W. Bryn Mawr Ave., Suite 1150, Chicago, IL 60631.

From the 1997 *Uniform Building Code* (UBC)[1] to the 2015 *International Building Code* (IBC),[2] the required quantity of confinement spiral ρ_s for 14 in. (350 mm) square prestressed concrete piles was capped at 0.021. This upper bound appears to be related to conclusions made by Banerjee et al.,[3] who found that 14 in. piles with a quantity of confinement spiral ρ_s greater than 0.020 were expected to have "virtually unlimited curvature capacity."[4] The usability of the curvature capacity was recently brought into question by Sritharan et al.[5] based on results obtained while performing a parametric study of pile ductility. Their research was funded by PCI and aimed at developing updated minimum spiral confinement equations intended for inclusion in the update of the PCI Prestressed Concrete Piling Committee's "Recommended Practice for Design, Manufacture, and Installation of Prestressed Concrete Piling"[6] and for possible consideration during future code development deliberations. When reviewing their research results, Sritharan et al. were concerned about the significant drop in moment capacity that occurs when the pile's cover spalls as part of the pile hinge process. In response, the researchers established a threshold of 40% as the maximum permitted drop in moment capacity that they would permit for 14 in. piles. For cases where the 40% drop was exceeded, published results are not available and the researchers recommended against the use of these piles. Because the percent drop is related to the axial load on the pile, the 40% drop was found by the researchers to occur in some cases when the axial load exceeded $0.2 f_c' A_g$, where f_c' is the specified 28-day concrete strength and A_g is the gross cross-sectional

area, or 20% of the nominal concrete compressive capacity of the 14 in. prestressed concrete pile.

The 2018 IBC[7] and the American Concrete Institute's *Building Code Requirements for Structural Concrete (ACI 318-19) and Commentary (ACI 318-19R)*[8] have now adopted the updated confinement equations developed by Sritharan et al.[5] and have also adopted axial load limits as suggested by these researchers. For seismic design categories C through F, IBC section 1810.3.8.3.4 and ACI 318-19 section 18.13.5.10.6 limit the factored axial load for all square prestressed concrete piles to $0.2 f'_c A_g$. Unfortunately, this limit prohibits the use of some commonly used 14 in. (350 mm) square prestressed concrete pile configurations in areas of moderate to high seismicity. The PCI Prestressed Concrete Piling Committee[6] has also adopted the updated confinement equations and axial load limits, but this PCI committee publication assumes that performance-based design will be used when the axial load limits are exceeded. Performance-based design of foundation elements is not explicitly codified in the 2018 IBC[7] and ACI 318-19,[8] making implementation an arduous task at best, possibly requiring the use of alternative means and methods provisions in some cases.

The basis of the limit on axial load described earlier can be explained with reference to **Fig. 1**, excerpted from Fanous et al.[9] In Fig. 1, a drop in moment capacity after the first peak moment and subsequent to reaching the second peak moment is evident. The results showed that the percent moment drop is related to the applied axial load used during moment-curvature analysis. Fanous et al.[9] suggested that this drop should be limited to approximately 40% of the first peak moment, and that the most effective way of managing the desired limit on the drop in moment was to limit the axial load. Therefore, axial load limits were recommended for the 14 in. (350 mm) pile to prevent loss in moment relative to the first peak moment in excess of approximately 40% based on the pile configurations considered (that is, 14 in. square piles with 2 in. [50.8 mm] cover and round spiral). Avoiding the 40% drop in moment reportedly correlated well with maintaining a response in which the curvature at the initiation of tension cracking ϕ_{cr} is less than the curvature associated with the initiation of unconfined concrete spalling ϕ_{sp}, where strain in the outermost unconfined compression fiber equal to 0.004 is taken as the value that spalling would initiate. According to Sritharan et al.,[5] "the reason for imposing this condition is that the magnitude of the moment drop due to spalling of the cover concrete is significant when $\phi_{sp} > \phi_{cr}$." Note that current codes do not require the curvature associated with the initiation of unconfined concrete spalling ϕ_{sp} to be greater than the curvature at the initiation of tension cracking ϕ_{cr} for seismic design and that the implementation of this requirement was selected to attempt to control the moment drop associated with seismic hinging.

It should be noted that Fanous et al.[9] do not appear to define or study the rationale for the concern or to determine if the moment drop would actually result in poor performance of the subject piling. Rather, the authors note that larger moment

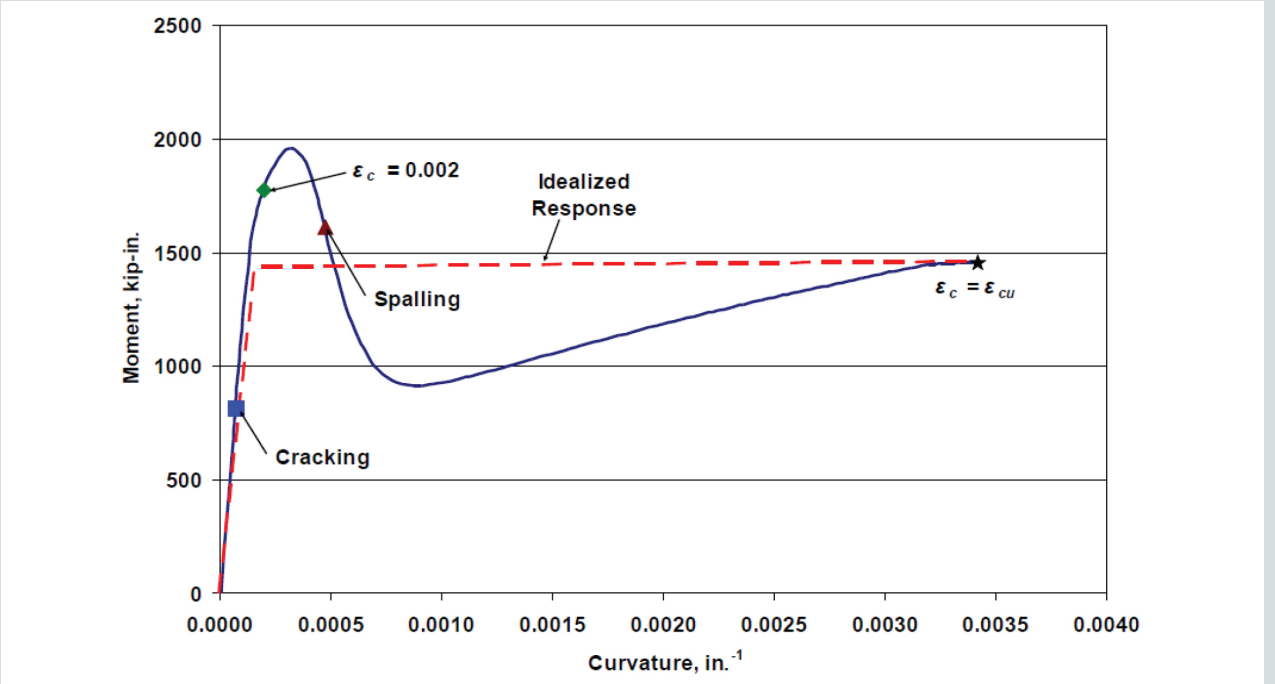

Figure 1. Moment-curvature relationship for a 14 in. square pile with specified concrete strength f'_c of 6000 psi, effective prestress f_{pc} of 1200 psi, and a 0.2 axial load ratio. Source: Reproduced by permission from Fanous et al. (2010, Fig. 3.30). Note: f'_c = specified 28-day strength of the concrete; f_{pc} = effective prestress in the pile; ε_c = strain in concrete; ε_{cu} = ultimate strain in concrete. 1 in. = 25.4 mm; 1 kip-in. = 0.113 kN-m; 1 psi = 6.895 kPa.

drops were deemed to be "unacceptable for piles in seismic regions" and "the stability of the pile experiencing significant moment drop may not be dependable." The concern about moment drop expressed by the previous researchers was an opinion based on research related to Eurocode and not U.S. codes and standards. *Seismic Design of Concrete Buildings to Eurocode 8*[10] discusses the moment drop issue and states that the ultimate ductility capacity is typically taken as the ductility capacity when the moment drops 20% from its peak value. This makes sense for moment-curvature analysis (that is, moment rotation results) where the moment is continuing to decline down to an unpredictable value at failure. **Figure 2** shows that typical small diameter auger-cast piles may warrant such consideration; however, as shown in the same figure, 14 in. (350 mm) square prestressed concrete piles are not approaching an impending failure mechanism and do not perform as assumed by the Eurocode provision. The Eurocode-related publication recognizes that this may be the case when it refers to the ductility capacity related to the 20% moment drop as follows: "It may be assumed that it represents the flexural deformation capacity of a member. Actually, a member has additional capacity beyond the NC (Near Collapse) limit state. In principle, it is possible to model the moment-rotation relation beyond the ultimate rotation of the plastic hinge θ_u; however, there is lack of data on the descending branch of the moment-rotation curve. Moreover, simulating the behavior beyond the NC limit state usually has only very limited practical value."

As will be discussed in the results section of this paper, 14 in. (350 mm) prestressed concrete piles have a second peak that can be shown to vary from 80% of the first peak to over 100% of the first peak moment in most cases. U.S. codes and standards committees are aware of the benefits and stability of the second peak moment that occurs for prestressed piles used as lateral-force-resisting elements and these committees have already established a vetted means to account for the first moment drop without applying an artificial axial load limit.

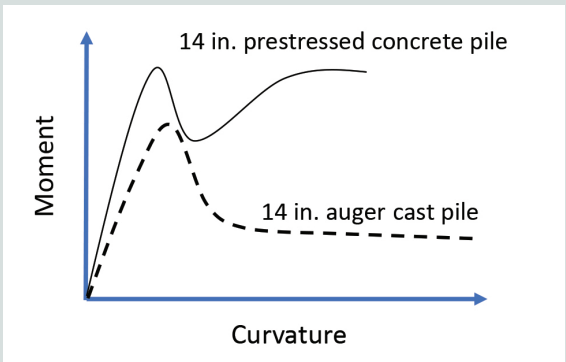

Figure 2. Comparison of typical moment-curvature relationships for a 14 in. square prestressed concrete pile and 14 in. auger cast pile with $0.2f'_cA_g$ applied axial load in both cases. Note: A_g = gross cross-sectional area; f'_c = specified 28-day strength of the concrete. 1 in. = 25.4 mm.

Current practice in the United States

It is well established in U.S. codes and standards that moment-curvature curves for prestressed concrete piles are very stable and unique in their response characteristics. Although building standards such as American Society of Civil Engineers (ASCE) Structural Engineering Institute's (SEI's) *Seismic Evaluation and Retrofit of Existing Buildings* ASCE/SEI 41-17[11] present recommendations on modeling building elements with moment drops leading to failure, building piles are designed to respond elastically to the design earthquake and thus modeling prestressed concrete pile ductility response is not a primary focus of these standards. On the other hand, in California, where seismic design is paramount, prestressed concrete pile ductility modeling provisions have been incorporated into the California Building Code through "Marine Oil Terminal Engineering and Maintenance Standards."[12] These provisions apply when prestressed concrete piles are the entire lateral-force-resisting system for marine oil terminal pier and wharf structures. Regarding moment-curvature analysis and ductility modeling of prestressed concrete piles, the California Building Code provisions are identical to what is presented in ASCE 61-14[13] for piers and wharfs and in *Port of Long Beach Wharf Design Criteria*.[14] Unlike the philosophy for building piles, because the moment-curvature response of pier piles is critical to the intended ductility performance of the entire structure, related codes and standards must address pile ductility limits as part of their criteria. The same is true for codes and standards related to bridge design in areas of high seismicity.

Port of Long Beach Wharf Design Criteria[14] provides an overview of how moment-curvature response is conservatively modeled for prestressed concrete piles. **Figure 3** is a generalized moment-curvature plot, which is useful in describing the Port of Long Beach[14] model. It should be noted that a fictitious axial load limit is not established. Rather, the

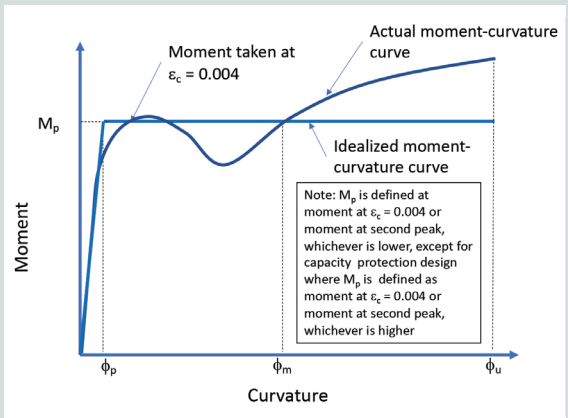

Figure 3. Typical moment-curvature model for prestressed concrete pile. Source: Adapted from Port of Long Beach (2015). Note: M_p = plastic or maximum moment on the bilinear idealized moment-curvature curve; ε_c = strain in concrete; ϕ_m = maximum curvature; ϕ_p = plastic curvature; ϕ_u = ultimate curvature.

California Building Code,[12] ASCE 61-14,[13] and *Port of Long Beach Wharf Design Criteria*[14] use energy dissipation penalties by reducing the moment and not the ultimate curvature. Specifically, if the second peak moment exceeds the first peak moment, the moment-curvature curve is taken as the bilinear curve shown with a maximum moment M_p associated with the first peak moment on the curve. If the second peak moment is less than the first peak moment, the moment-curvature curve is taken as the bilinear curve shown but with a maximum moment M_p equal to the second peak moment on the curve. In other words, if a moment drop occurs and the moment-curvature curve does not return to a (second peak) maximum moment equal to or greater than the value associated with the first peak, the bilinear moment-curvature curve shall be taken with a maximum moment equal to the second peak moment. This simple approach penalizes the design by dissipating less energy (that is, energy dissipation is related to the area under the moment-curvature curve), which also results in a larger displacement demand for the structure. The larger displacement demand yields larger second-order effects as well; however, it should be noted that the ultimate curvature capacity ϕ_u is not decreased. In addition, as previously stated, axial load limits are not established, which is contrary to recommendations from Fanous et al.[9] To avoid any confusion, it should be noted that performance-based design typically does use lateral load drops exceeding 20% as the limit when using pushover analysis for the lateral-force-resisting system. This limit is not relevant to the topic addressed in this paper as it is meant to prevent progressive collapse of the lateral-force-resisting system caused by excessive second-order effects (that is, axial load P and pile deflection Δ, or P-Δ, effects).

Bridge codes and standards use performance-based design approaches that are very similar to those used in the pier and wharf industry, with notable variations. For example,

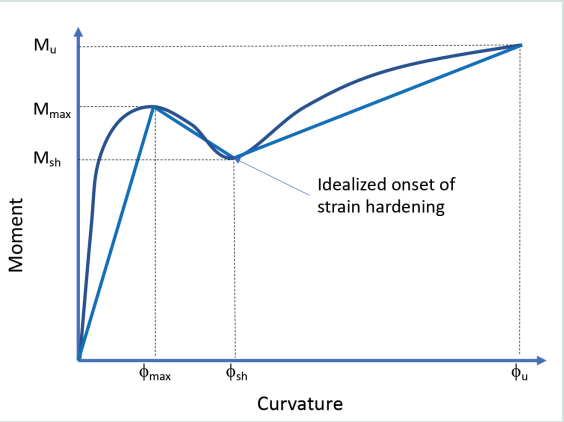

Figure 4. Trilinear moment-curvature model for prestressed concrete pile. Source: Adapted from South Carolina Department of Transportation (2008). Note: M_{max} = maximum moment; M_{sh} = moment at strain hardening; M_u = ultimate moment; ϕ_{max} = maximum curvature; ϕ_{sh} = curvature at strain hardening; ϕ_u = ultimate curvature.

in addition to simple bilinear moment-curvature models for prestressed concrete piles often used in the industry, codes and standards such as the South Carolina Department of Transportation *SCDOT Seismic Design Criteria*[15] also allow the engineer to directly model the trilinear behavior of the pile to account for moment loss (**Fig. 4**). These models may be considered more accurate in regard to capturing the maximum and minimum moments of the moment-curvature curve and global stability of the structure is more accurately accounted for when trilinear models are used. In addition to trilinear models, modern software allows for moment-curvature curves made of many points and, in these cases, not only strength but also stiffness is more accurately represented.

Procedure

The primary focus of this study was to analyze through modeling the moment-curvature response of 14 in. (350 mm) square prestressed concrete piles with varying axial loads exceeding $0.2 f'_c A_g$.

Both round and square spiral configurations, enclosing round and square strand patterns respectively, with 2 and 3 in. (50.8 and 76.2 mm) of cover were considered. Standard use in the industry limits the scope of the study to six- and eight-strand configurations with effective prestress after losses between 700 and 1200 psi (4830 and 8270 kPa). Concrete compressive strengths between 5000 and 8000 psi (34,500 and 55,200 kPa) were considered. Prestressing strands were assumed to conform to ASTM A416.[15] Plain wire reinforcement was assumed to conform to ASTM A1064.[16] In this study, and as required by ASTM A1064, wire reinforcement was assumed to have a yield stress of 65 ksi (448 MPa) and an ultimate stress of 75 ksi (517 MPa). For the purposes of this study, nominal rather than expected material properties were assumed.

Performance-based design codes often require the use of expected material properties when performing moment-curvature analyses. All moment-curvature analysis results presented in this report were obtained using SAP2000, a structural analysis and design software. SAP2000 has its own built-in material modeling and moment-curvature analysis methodologies that are well recognized by both academic and industry practice. Prestressing strands and wire reinforcement are modeled using nonlinear material models. Unconfined and confined concrete are modeled using the model from Mander et al.[18] (**Fig. 5**). Readers seeking more information regarding material models considered in this paper are referred to Ryan and Mays.[19]

A distinction should be noted between analysis tools used for the research presented in this paper and those used in the prior study. The analysis program chosen by Fanous et al.[9] had element limitations and, therefore, the research team created special elements to attempt to model the full cross-sectional behavior. In addition, the geometries considered were limited to round spiral configurations with 2 in.

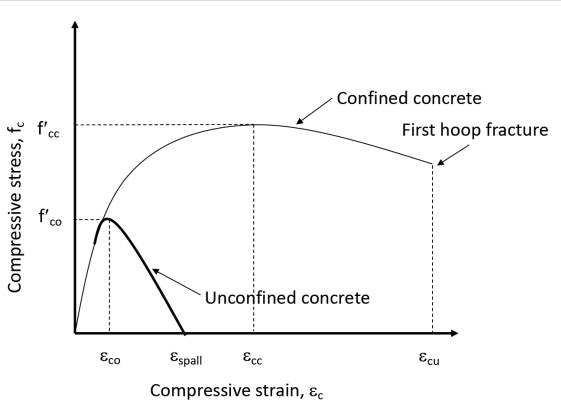

Figure 5. Mander's model for unconfined and confined concrete. Source: Adapted from Mander et al. (1988). Note: f'_{cc} = ultimate stress in confined concrete; f'_{co} = stress in unconfined concrete; ε_{cc} = strain in confined concrete at peak stress; ε_{co} = strain in unconfined concrete at peak stress; ε_{cu} = ultimate strain in concrete; ε_{spall} = strain at unconfined concrete spalling.

(50.8 mm) of cover. Square confinement and square strand configurations were not considered by the previous research. The previous research authors do not suggest that fiber models created for their study were validated for the correct number of fiber elements nor compared with other software used in the industry to validate the accuracy of the moment drop calculated during the study. Fanous et al.[9] compared results obtained from the two program options used in the previous research (**Fig. 6**). The authors state that the figure shows "fairly similar behavior confirming the accuracy of both programs." This appears to be true for ultimate curvature, but when comparing the values for initial peak moment and moment after initial loss in strength, the analyzed values differ by a factor of approximately 1.5 and 2.0, respectively. Because conclusions related to applying axial load limits are drawn almost entirely from these initial portions of the moment-curvature response, greater scrutiny of the model is warranted.

All moment-curvature analysis results presented in this paper were obtained using section designer within SAP2000. No elements were developed by the research team to model the pile cross sections, as SAP2000 has required element models available within the program, and these elements have been fully tested for use as part of the subject research. **Figure 7** shows a typical pile cross section modeled in SAP2000. Prior to performing the parametric study, fiber models with rectangular and cylindrical configurations were tested for convergence with exact integration solutions. **Figures 8** and **9** show typical fiber element configurations tested during the convergence study. It was determined that in all cases, 30 × 30 rectangular and 30 × 20 cylindrical configurations always matched the exact integration solution. The cylindrical fiber configuration required fewer elements and was thus favored for circular confinement sections. The rectangular fiber configuration was favored for square confinement sections.

Parametric study parameters

Using the material models discussed in the previous section for the prestressing strand, spiral reinforcement, unconfined concrete, and confined concrete, a moment-curvature-related parametric study of 14 in. (350 mm) square prestressed pile

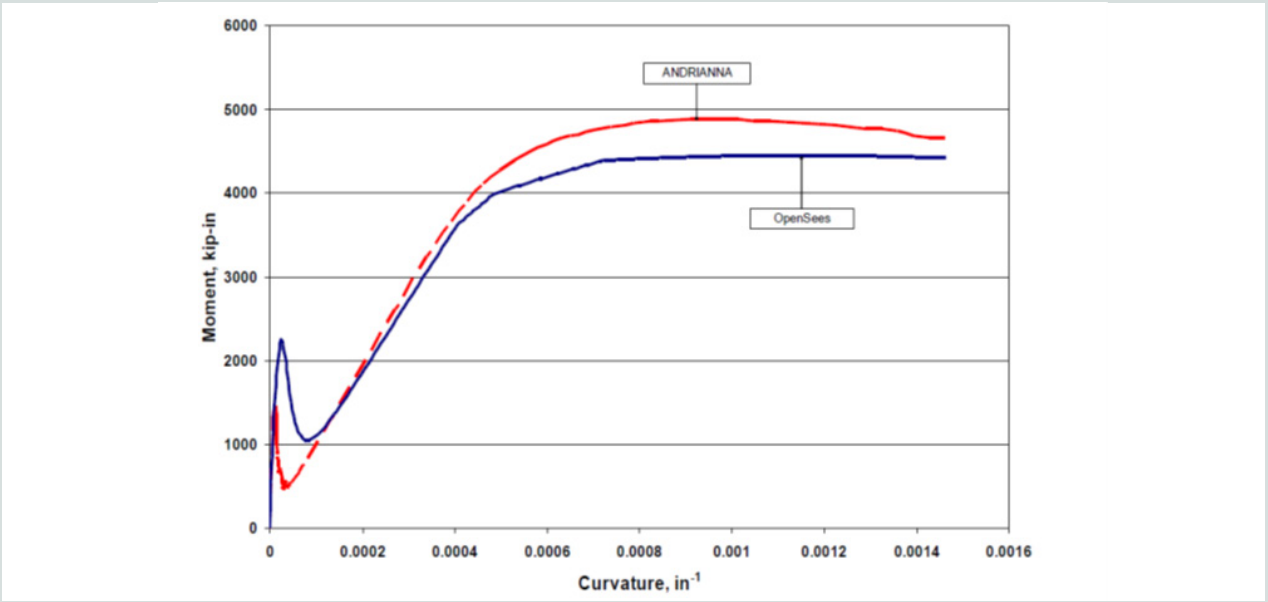

Figure 6. A comparison of moment-curvature response results obtained from two separate programs. Source: Reproduced by permission from Fanous et al. (2010, Fig. 3.11). Note: 1 in. = 25.4 mm; 1 kip-in. = 0.113 kN-m.

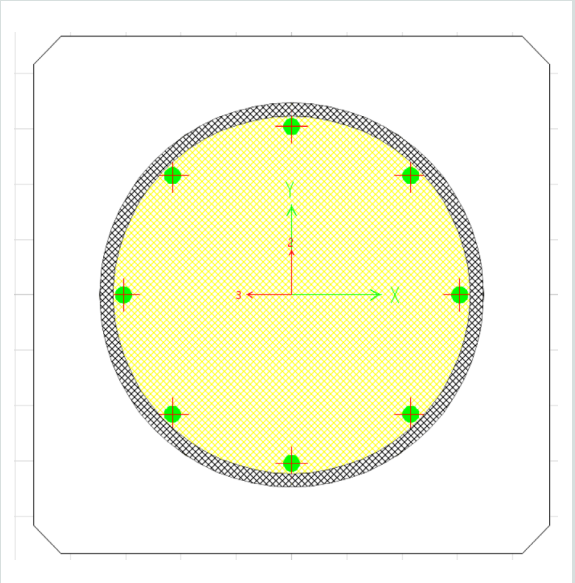

Figure 7. Typical cross-sectional model showing strands, spiral, confined concrete, and unconfined concrete properties in SAP2000.

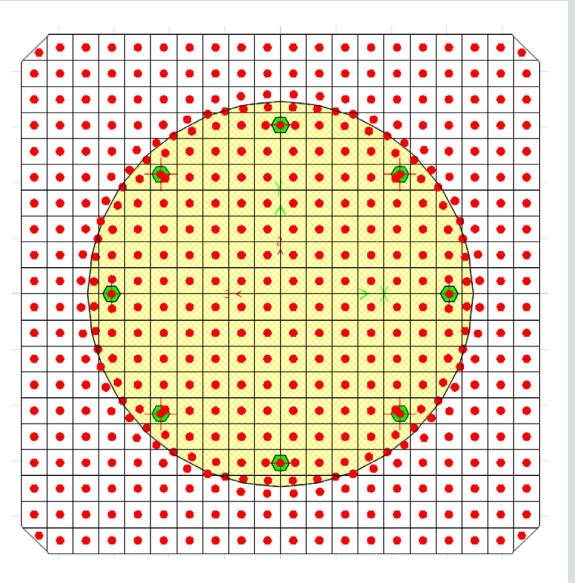

Figure 8. Typical rectangular fiber model (20 × 20 shown).

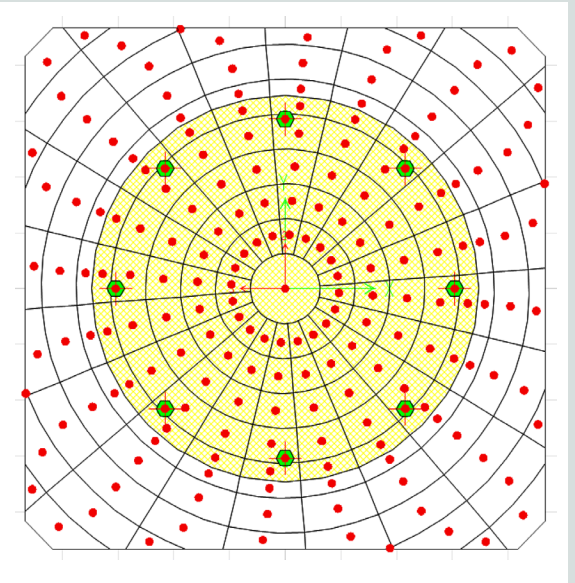

Figure 9. Typical cylindrical fiber model (20 × 10 shown).

configurations was performed. The study was limited to pile cross sections and initial prestress levels commonly used in the United States. The following parameters were considered:

- normalweight concrete with concrete compressive strength f_c' between 5000 and 8000 psi (34,500 and 55,200 kPa)
- concrete cover to the spiral reinforcement between 2 and 3 in. (50.8 and 76.2 mm)
- effective prestress after losses f_{pc} between 700 and 1200 psi (4830 and 8270 kPa)
- axial load P between 0.2 $f_c' A_g$ and 0.35 $f_c' A_g$
- six- and eight-strand circular configurations (with circular spiral confinement wire)
- six- and eight-strand square configurations (with square confinement wire)

The amount of spiral reinforcement modeled was determined using the prescriptive requirements of the PCI Prestressed Concrete Piling Committee.[6] For piles using a circular prestressed reinforcement configuration, the quantity of confinement spiral ρ_s provided was taken as:

$$\rho_s = 0.06\left(\frac{f_c'}{f_{yh}}\right)\left(2.8+\frac{1.25P}{0.53f_c'A_g}\right) \quad (1)$$

where

f_{yh} = yield strength of spiral reinforcement

For piles with a square prestressed reinforcement configuration, the total cross-sectional area of transverse reinforcement provided separately in each direction, including crossties where applicable A_{sh} was taken as:

$$A_{sh} = 0.04sh_c\left(\frac{f_c'}{f_{yh}}\right)\left(2.8+\frac{1.25P}{0.53f_c'A_g}\right) \quad (2)$$

where

s = longitudinal spacing of the transverse steel

h_c = confined concrete side dimension defined by transverse steel dimension

W10 and W12 wire were used exclusively for spiral wire during the study. Spacing of the spiral was used to proportion the quantity of confinement spiral ρ_s and the total cross-sectional area of transverse reinforcement A_{sh} to match minimum prescriptive values calculated using Eq. (1) and (2). Spacing of the spiral was also verified to be less than the maximum recommended spacing presented in the PCI Prestressed Concrete Piling Committee's recommended practice,[6] such that the spacing for all models did not exceed the minimum of:

- $\frac{1}{5}$ of the smallest pile dimension
- six strand diameters
- 6 in. (152 mm)

As previously discussed, axial load limits were recommended by Fanous et al.[9] for the 14 in. (350 mm) pile to prevent loss in moment relative to the first peak moment in excess of approximately 40% based on pile configurations considered (that is, 14 in. square piles with 2 in. [50.8 mm] cover and round spiral). As such, this paper presents the results of the parametric study as related to the drop in moment after the first peak moment occurs during moment-curvature analysis. This section of the paper accepts the premise that the 40% moment drop is actually a concern and presents the results of a thorough study (as recommended by Fanous et al.[9]) of axial loads and pile geometries related to 14 in. prestressed concrete piles in seismic areas as needed to provide designers a practical response to the new and arbitrary axial load limit established by the previous researchers.

Because the moment drop, or percent moment drop, after the first peak moment is the critical data point to be recorded during this study, it was recorded for every moment-curvature analysis performed. The second peak moment is also a data point of interest because the second peak moment often returns close to the initial peak moment value. The second peak moment ensures section stability and seismic energy dissipation. More importantly, the second peak should make the initial moment drop less of a concern as the descending branch of the moment-curvature curve does not continue downward in an unreliable manner with limited energy dissipation capability. For the reasons discussed above, the research team has recorded the three moment values for all moment-curvature analyses (**Fig. 10**).

The curvature values associated with the three moment values were not recorded during the study; however, each analysis was checked to ensure that the available curvature ductility capacity was greater than 18 for all cases as required by Fanous et al.[9] and the PCI Prestressed Concrete Piling Committee.[6]

For discussion of the results presented in this chapter, it is convenient to define two moment ratios: percent drop and percent return.

Percent drop *%Drop* is the ratio of the minimum moment that occurs after $M_{peak,1}$ on the moment-curvature curve M_{drop} to the first maximum moment that occurs on the moment-curvature curve $M_{peak,1}$ and percent return *%Return* is the ratio of the second maximum moment that occurs after M_{drop} on the moment-curvature curve $M_{peak,2}$ to the first maximum moment that occurs on the moment-curvature curve $M_{peak,1}$. Percent drop *%Drop* was used to compare the SAP2000 model results described herein with results from Fanous et al.[9] The previous study limited *%Drop* to no less than 60%. In other words, if the first maximum moment that occurs on the moment-curvature curve $M_{peak,1}$ was reduced by more than 40%, the combination of pile cross section, prestress, and axial load was determined to be unsuitable and *%Return* was not reported. Recommended axial load limits were, in part, calibrated based on that criterion. Based on *%Drop*, this study showed that increased axial load limits can be validated using an improved SAP2000 model while remaining consistent with methodology used by Fanous et al.[9] The SAP2000 model contains more realistic and industry-proven fiber elements than those used in the previous study. SAP2000 is also used commercially by practicing engineers to model prestressed pile hinging.

Percent return *%Return* is the measure of proximity to the first peak moment that a pile can be expected to achieve during stable hinging behavior. Percent return *%Return* is less than 1.0 when the second peak moment is less than the first peak moment. Percent return *%Return* is equal to 1.0 when the second peak moment is equal to the first peak moment. Percent return *%Return* is greater than 1.0 when the pile second peak moment is greater than the first peak moment. Percent return *%Return* has been included as a basis for possible modification of the previously accepted methodology for axial load limit.

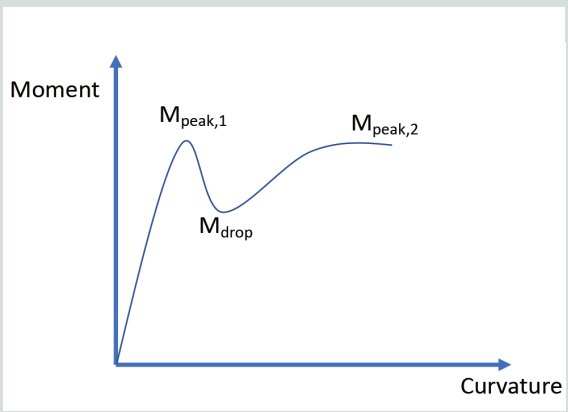

Figure 10. Three data points recorded during moment-curvature analysis. Note: M_{drop} = minimum moment that occurs after $M_{peak,1}$ on the moment-curvature curve; $M_{peak,1}$ = first maximum moment that occurs on the moment-curvature curve; $M_{peak,2}$ = second maximum moment that occurs after M_{drop} on the moment-curvature curve.

Results: 14 in. square piles with 2 in. cover

For this study, the aim of the research team was to perform a moment-curvature-related parametric study of 14 in. (350 mm) prestress pile configurations limited to pile cross sections and initial prestress levels commonly used in the United States. For each configuration considered, the first maximum moment that occurs on the moment-curvature curve $M_{peak,1}$, the minimum moment that occurs after $M_{peak,1}$ on the moment-curvature curve M_{drop}, and the second maximum moment that occurs after M_{drop} on the moment-curvature curve $M_{peak,2}$ were recorded. **Tables 1** through **10** present the results provided by the moment-curvature analysis for the 160 primary cases considered in this study.

A few practical points should be made regarding typical 14 in. (350 mm) piles. In practical design, the strands are typically pretensioned to 75% of the ultimate strength of prestressing strands f_{pu} and the piles normally exhibit losses around 15%. The baseline cases for this study consist of the most common pile strand configurations used in practice, which are the six-strand and eight-strand patterns, using ½ in. (12.7 mm) diameter strands (cross-sectional area of spiral reinforcement A_{sp} is 0.153 in.^{2} [98.7 mm^2] per strand). Losses for the baseline cases are assumed to be 15%. The six-strand baseline case has an effective prestress very close to the 700 psi (4830 kPa) minimum value considered in the study. Similarly, the eight-strand baseline case has an effective prestress very close to the 1200 psi (8270 kPa) maximum value considered. The data presented in Tables 1 through 10 are for the bounds considered in the study; however, it should be noted that the results from the baseline cases did not noticeably change from the adjacent upper- and lower-bound results; as such, and to avoid reader confusion, the results for the baseline cases are not presented as separate cases in this paper. It should be noted that 1200 psi effective prestress, as defined in the maximum prestress cases, would be difficult to achieve in practice using the ½ in. strand configurations discussed earlier and accounting for losses. There may be occasions where adding strand, using different strand sizes, and reducing the initial tension in the strands from 75% of ultimate strength of the prestressing strand f_{pu} could achieve a performance objective, however, the designer should provide clear instructions for the producer to avoid confusion and increased costs associated with additional steel.

Based solely on the results presented in Tables 1 through 4, it can be argued that for circular spiral and strand configurations, $0.25 f_c' A_g$ is a more appropriate axial load limit when the effective prestress is near 1200 psi (8270 kPa). For circular spiral and strand configurations, $0.30 f_c' A_g$ is a more appropriate axial load limit when the effective prestress is near 700 psi (4830 kPa), at least up to a compressive concrete strength f_c' of 7000 psi (48,300 kPa).

Table 1. Results of moment-curvature analysis for 14 in. square pile with eight strands, circular W10 confinement, 0.5 in. diameter strand, and 1200 psi effective prestress

f_c', ksi	Multiplier $f_c' A_g$	$M_{peak,1}$, kip-in.	M_{drop}, kip-in.	$M_{peak,2}$, kip-in.	%Drop	%Return
5	0.20	1650	1120	1490	68	90
6	0.20	1890	1270	1630	67	86
7	0.20	2240	1350	1720	60	77
8	0.20	2460	1490	1860	61	76
5	0.25	1680	1090	1510	65	90
6	0.25	1940	1230	1660	63	86
7	0.25	2280	1310	1760	57	77
8	0.25	2530	1450	1900	57	75
5	0.30	1700	1020	1500	60	88
6	0.30	1970	1170	1670	59	85
7	0.30	2270	1230	1770	54	78
8	0.30	2540	1370	1900	54	75
5	0.35	1700	950	1500	56	88
6	0.35	1970	1100	1660	56	84
7	0.35	2240	1120	1750	50	78
8	0.35	2500	1240	1900	50	76

Note: A_g = gross cross-sectional area; f_c' = specified 28-day strength of the concrete; M_{drop} = minimum moment that occurs after $M_{peak,1}$ on the moment-curvature curve; $M_{peak,1}$ = first maximum moment that occurs on the moment-curvature curve; $M_{peak,2}$ = second maximum moment that occurs after M_{drop} on the moment-curvature curve; *%Drop* = ratio of M_{drop} to $M_{peak,1}$; *%Return* = ratio of $M_{peak,2}$ to $M_{peak,1}$. 1 in. = 25.4 mm; 1 kip-in. = 0.113 kN-m; 1 psi = 6.895 kPa; 1 ksi = 6.895 MPa; W10 = MW65.

Table 2. Results of moment-curvature analysis for 14 in. square pile with eight strands, circular W10 confinement, 0.5 in. diameter strand, and 700 psi effective prestress

f'_c, ksi	Multiplier $f'_c A_g$	$M_{peak,1}$, kip-in.	M_{drop}, kip-in.	$M_{peak,2}$, kip-in.	%Drop	%Return
5	0.20	1700	1150	1500	68	88
6	0.20	2030	1260	1640	62	81
7	0.20	2140	1440	1780	67	83
8	0.20	2350	1570	1900	67	81
5	0.25	1730	1130	1540	65	89
6	0.25	2050	1220	1660	60	81
7	0.25	2210	1420	1820	64	82
8	0.25	2440	1540	1950	63	80
5	0.30	1730	1080	1540	62	89
6	0.30	2050	1160	1670	57	81
7	0.30	2270	1360	1830	60	81
8	0.30	2510	1490	1980	59	79
5	0.35	1740	1010	1520	58	87
6	0.35	2020	1050	1650	52	82
7	0.35	2280	1280	1810	56	79
8	0.35	2540	1400	1950	55	77

Note: A_g = gross cross-sectional area; f'_c = specified 28-day strength of the concrete; M_{drop} = minimum moment that occurs after $M_{peak,1}$ on the moment-curvature curve; $M_{peak,1}$ = first maximum moment that occurs on the moment-curvature curve; $M_{peak,2}$ = second maximum moment that occurs after M_{drop} on the moment-curvature curve; *%Drop* = ratio of M_{drop} to $M_{peak,1}$; *%Return* = ratio of $M_{peak,2}$ to $M_{peak,1}$. 1 in. = 25.4 mm; 1 kip-in. = 0.113 kN-m; 1 psi = 6.895 kPa; 1 ksi = 6.895 MPa; W10 = WM65.

Table 3. Results of moment-curvature analysis for 14 in. square pile with six strands, circular W10 confinement, 0.5 in. diameter strand, and 1200 psi effective prestress

f'_c, ksi	Multiplier $f'_c A_g$	$M_{peak,1}$, kip-in.	M_{drop}, kip-in.	$M_{peak,2}$, kip-in.	%Drop	%Return
5	0.20	1610	990	1210	61	75
6	0.20	1850	1140	1350	62	73
7	0.20	2070	1270	1470	61	71
8	0.20	2290	1400	1600	61	70
5	0.25	1650	960	1240	58	75
6	0.25	1900	1120	1390	59	73
7	0.25	2150	1250	1510	58	70
8	0.25	2390	1380	1660	58	69
5	0.30	1660	900	1230	54	74
6	0.30	1900	1060	1390	56	73
7	0.30	2200	1190	1520	54	69
8	0.30	2450	1330	1670	54	68
5	0.35	1650	820	1190	50	72
6	0.35	1930	980	1360	51	70
7	0.35	2200	1110	1490	50	68
8	0.35	2470	1230	1640	50	66

Note: A_g = gross cross-sectional area; f'_c = specified 28-day strength of the concrete; M_{drop} = minimum moment that occurs after $M_{peak,1}$ on the moment-curvature curve; $M_{peak,1}$ = first maximum moment that occurs on the moment-curvature curve; $M_{peak,2}$ = second maximum moment that occurs after M_{drop} on the moment-curvature curve; *%Drop* = ratio of M_{drop} to $M_{peak,1}$; *%Return* = ratio of $M_{peak,2}$ to $M_{peak,1}$. 1 in. = 25.4 mm; 1 kip-in. = 0.113 kN-m; 1 psi = 6.895 kPa; 1 ksi = 6.895 MPa; W10 = MW65.

Table 4. Results of moment-curvature analysis for 14 in. square pile with six strands, circular W10 confinement, 0.5 in. diameter strand, and 700 psi effective prestress

f'_c, ksi	Multiplier $f'_c A_g$	$M_{peak,1}$, kip-in.	M_{drop}, kip-in.	$M_{peak,2}$, kip-in.	%Drop	%Return
5	0.20	1640	1050	1250	64	76
6	0.20	1870	1190	1380	64	74
7	0.20	2090	1320	1500	63	72
8	0.20	2350	1540	1540	66	66
5	0.25	1680	1020	1280	61	76
6	0.25	1930	1180	1430	61	74
7	0.25	2180	1310	1560	60	72
8	0.25	2460	1320	1590	54	65
5	0.30	1700	980	1290	58	76
6	0.30	1970	1140	1440	58	73
7	0.30	2200	1270	1580	58	72
8	0.30	2500	1260	1600	50	64
5	0.35	1700	920	1280	54	75
6	0.35	1980	1060	1430	54	72
7	0.35	2250	1190	1550	53	69
8	0.35	2470	1140	1570	46	64

Note: A_g = gross cross-sectional area; f'_c = specified 28-day strength of the concrete; M_{drop} = minimum moment that occurs after $M_{peak,1}$ on the moment-curvature curve; $M_{peak,1}$ = first maximum moment that occurs on the moment-curvature curve; $M_{peak,2}$ = second maximum moment that occurs after M_{drop} on the moment-curvature curve; *%Drop* = ratio of M_{drop} to $M_{peak,1}$; *%Return* = ratio of $M_{peak,2}$ to $M_{peak,1}$. 1 in. = 25.4 mm; 1 kip-in. = 0.113 kN-m; 1 psi = 6.895 kPa; 1 ksi = 6.895 MPa; W10 = MW65.

Table 5. Results of moment-curvature analysis for 14 in. square pile with eight strands, square W12 confinement, 0.5 in. diameter strand, and 1200 psi effective prestress

f'_c, ksi	Multiplier $f'_c A_g$	$M_{peak,1}$, kip-in.	M_{drop}, kip-in.	$M_{peak,2}$, kip-in.	%Drop	%Return
5	0.20	1840	1330	1880	72	102
6	0.20	2070	1490	1970	72	95
7	0.20	2320	1680	2130	72	92
8	0.20	2540	1830	2230	72	88
5	0.25	1860	1300	1890	70	102
6	0.25	2110	1470	1940	70	92
7	0.25	2360	1670	2180	71	92
8	0.25	2590	1810	2210	70	85
5	0.30	1840	1250	1850	68	101
6	0.30	2100	1410	1900	67	90
7	0.30	2360	1630	2130	69	90
8	0.30	2600	1770	2130	68	82
5	0.35	1790	1160	1830	65	102
6	0.35	2060	1310	1850	64	90
7	0.35	2320	1540	2070	66	89
8	0.35	2570	1660	2060	65	80

Note: A_g = gross cross-sectional area; f'_c = specified 28-day strength of the concrete; M_{drop} = minimum moment that occurs after $M_{peak,1}$ on the moment-curvature curve; $M_{peak,1}$ = first maximum moment that occurs on the moment-curvature curve; $M_{peak,2}$ = second maximum moment that occurs after M_{drop} on the moment-curvature curve; *%Drop* = ratio of M_{drop} to $M_{peak,1}$; *%Return* = ratio of $M_{peak,2}$ to $M_{peak,1}$. 1 in. = 25.4 mm; 1 kip-in. = 0.113 kN-m; 1 psi = 6.895 kPa; 1 ksi = 6.895 MPa; W12 = MW77.

Table 6. Results of moment-curvature analysis for 14 in. square pile with eight strands, square W12 confinement, 0.5 in. diameter strand, and 700 psi effective prestress

f'_c, ksi	Multiplier $f'_c A_g$	$M_{peak,1}$, kip-in.	M_{drop}, kip-in.	$M_{peak,2}$, kip-in.	%Drop	%Return
5	0.20	1840	1450	1890	79	103
6	0.20	2050	1610	1980	79	97
7	0.20	2260	1780	2170	79	96
8	0.20	2450	1910	2240	78	91
5	0.25	1860	1420	1900	76	102
6	0.25	2090	1580	1920	76	92
7	0.25	2320	1780	2180	77	94
8	0.25	2540	1900	2180	75	86
5	0.30	1850	1400	1860	76	101
6	0.30	2110	1530	1920	73	91
7	0.30	2360	1750	2140	74	91
8	0.30	2590	1870	2160	72	83
5	0.35	1840	1320	1850	72	101
6	0.35	2110	1470	1890	70	90
7	0.35	2370	1690	2110	71	89
8	0.35	2600	1800	2100	69	81

Note: A_g = gross cross-sectional area; f'_c = specified 28-day strength of the concrete; M_{drop} = minimum moment that occurs after $M_{peak,1}$ on the moment-curvature curve; $M_{peak,1}$ = first maximum moment that occurs on the moment-curvature curve; $M_{peak,2}$ = second maximum moment that occurs after M_{drop} on the moment-curvature curve; *%Drop* = ratio of M_{drop} to $M_{peak,1}$; *%Return* = ratio of $M_{peak,2}$ to $M_{peak,1}$. 1 in. = 25.4 mm; 1 kip-in. = 0.113 kN-m; 1 psi = 6.895 kPa; 1 ksi = 6.895 MPa; W12 = MW77.

Table 7. Results of moment-curvature analysis for 14 in. square pile with six strands (strong axis), square W12 confinement, 0.5 in. diameter strand, and 1200 psi effective prestress

f'_c, ksi	Multiplier $f'_c A_g$	$M_{peak,1}$, kip-in.	M_{drop}, kip-in.	$M_{peak,2}$, kip-in.	%Drop	%Return
5	0.20	1650	1150	1560	70	95
6	0.20	1890	1300	1660	69	88
7	0.20	2130	1480	1780	69	84
8	0.20	2350	1610	1870	69	80
5	0.25	1680	1120	1670	67	99
6	0.25	1940	1280	1790	66	92
7	0.25	2200	1490	1920	68	87
8	0.25	2430	1620	2040	67	84
5	0.30	1680	1060	1800	63	107
6	0.30	1950	1230	1930	63	99
7	0.30	2210	1450	2080	66	94
8	0.30	2460	1590	2200	65	89
5	0.35	1650	980	1860	59	113
6	0.35	1910	1120	1890	59	99
7	0.35	2190	1360	2120	62	97
8	0.35	2440	1490	2130	61	87

Note: A_g = gross cross-sectional area; f'_c = specified 28-day strength of the concrete; M_{drop} = minimum moment that occurs after $M_{peak,1}$ on the moment-curvature curve; $M_{peak,1}$ = first maximum moment that occurs on the moment-curvature curve; $M_{peak,2}$ = second maximum moment that occurs after M_{drop} on the moment-curvature curve; *%Drop* = ratio of M_{drop} to $M_{peak,1}$; *%Return* = ratio of $M_{peak,2}$ to $M_{peak,1}$. 1 in. = 25.4 mm; 1 kip-in. = 0.113 kN-m; 1 psi = 6.895 kPa; 1 ksi = 6.895 MPa; W12 = MW77.

Table 8. Results of moment-curvature analysis for 14 in. square pile with six strands (strong axis), square W12 confinement, 0.5 in. diameter strand, and 700 psi effective prestress

f'_c, ksi	Multiplier $f'_c A_g$	$M_{peak,1}$, kip-in.	M_{drop}, kip-in.	$M_{peak,2}$, kip-in.	%Drop	%Return
5	0.20	1816	1414	1720	78	95
6	0.20	2030	1550	1840	76	91
7	0.20	2240	1720	1990	77	89
8	0.20	2450	1840	2100	75	86
5	0.25	1860	1410	1860	76	100
6	0.25	2080	1570	1970	75	95
7	0.25	2310	1760	2140	76	93
8	0.25	2530	1890	2250	75	89
5	0.30	1880	1380	1900	73	101
6	0.30	2110	1550	1950	73	92
7	0.30	2360	1740	2180	74	92
8	0.30	2580	1870	2200	72	85
5	0.35	1860	1330	1960	72	105
6	0.35	2110	1470	1910	70	91
7	0.35	2360	1670	2120	71	90
8	0.35	2600	1790	2150	69	83

Note: A_g = gross cross-sectional area; f'_c = specified 28-day strength of the concrete; M_{drop} = minimum moment that occurs after $M_{peak,1}$ on the moment-curvature curve; $M_{peak,1}$ = first maximum moment that occurs on the moment-curvature curve; $M_{peak,2}$ = second maximum moment that occurs after M_{drop} on the moment-curvature curve; *%Drop* = ratio of M_{drop} to $M_{peak,1}$; *%Return* = ratio of $M_{peak,2}$ to $M_{peak,1}$. 1 in. = 25.4 mm; 1 kip-in. = 0.113 kN-m; 1 psi = 6.895 kPa; 1 ksi = 6.895 MPa; W12 = MW77.

Table 9. Results of moment-curvature analysis for 14 in. square pile with six strands (weak axis), square W12 confinement, 0.5 in. diameter strand, and 1200 psi effective prestress

f'_c, ksi	Multiplier $f'_c A_g$	$M_{peak,1}$, kip-in.	M_{drop}, kip-in.	$M_{peak,2}$, kip-in.	%Drop	%Return
5	0.20	1630	1080	1430	66	88
6	0.20	1880	1230	1510	65	80
7	0.20	2120	1420	1650	67	78
8	0.20	2350	1560	1740	66	74
5	0.25	1660	1040	1510	63	91
6	0.25	1920	1210	1570	63	82
7	0.25	2180	1410	1760	65	81
8	0.25	2420	1560	1840	64	76
5	0.30	1650	980	1470	59	89
6	0.30	1920	1130	1510	59	79
7	0.30	2200	1360	1760	62	80
8	0.30	2450	1500	1780	61	73
5	0.35	1620	890	1430	55	88
6	0.35	1890	1030	1460	54	77
7	0.35	2180	1280	1700	59	78
8	0.35	2430	1400	1670	58	69

Note: A_g = gross cross-sectional area; f'_c = specified 28-day strength of the concrete; M_{drop} = minimum moment that occurs after $M_{peak,1}$ on the moment-curvature curve; $M_{peak,1}$ = first maximum moment that occurs on the moment-curvature curve; $M_{peak,2}$ = second maximum moment that occurs after M_{drop} on the moment-curvature curve; *%Drop* = ratio of M_{drop} to $M_{peak,1}$; *%Return* = ratio of $M_{peak,2}$ to $M_{peak,1}$. 1 in. = 25.4 mm; 1 kip-in. = 0.113 kN-m; 1 psi = 6.895 kPa; 1 ksi = 6.895 MPa; W12 = MW77.

Table 10. Results of moment-curvature analysis for 14 in. square pile with six strands (weak axis), square W12 confinement, 0.5 in. diameter strand, and 700 psi effective prestress

f'_c, ksi	Multiplier $f'_c A_g$	$M_{peak,1}$, kip-in.	M_{drop}, kip-in.	$M_{peak,2}$, kip-in.	%*Drop*	%*Return*
5	0.20	1700	1270	1530	75	90
6	0.20	1920	1390	1610	72	84
7	0.20	2140	1560	1810	73	85
8	0.20	2340	1700	1890	73	81
5	0.25	1740	1260	1530	72	88
6	0.25	1990	1410	1580	71	79
7	0.25	2220	1610	1820	73	82
8	0.25	2450	1730	1850	71	76
5	0.30	1760	1240	1500	70	85
6	0.30	2020	1390	1570	69	78
7	0.30	2280	1600	1780	70	78
8	0.30	2520	1720	1810	68	72
5	0.35	1770	1180	1470	67	83
6	0.35	2030	1330	1520	66	75
7	0.35	2290	1540	1740	67	76
8	0.35	2540	1660	1760	65	69

Note: A_g = gross cross-sectional area; f'_c = specified 28-day strength of the concrete; M_{drop} = minimum moment that occurs after $M_{peak,1}$ on the moment-curvature curve; $M_{peak,1}$ = first maximum moment that occurs on the moment-curvature curve; $M_{peak,2}$ = second maximum moment that occurs after M_{drop} on the moment-curvature curve; *%Drop* = ratio of M_{drop} to $M_{peak,1}$; *%Return* = ratio of $M_{peak,2}$ to $M_{peak,1}$. 1 in. = 25.4 mm; 1 kip-in. = 0.113 kN-m; 1 psi = 6.895 kPa; 1 ksi = 6.895 MPa; W12 = MW77.

Based solely on the results presented in Tables 5 through 10, it can be argued that for square spiral and strand configurations, $0.35A_g$ is a more appropriate axial load limit when the effective prestress is between 700 and 1200 psi (4830 and 8270 kPa). The only exception was for the singly symmetric six-strand case (weak axis; Table 9) where $0.30 f'_c A_g$ is a more appropriate axial load limit when the effective prestress is near 1200 psi.

Results: 14 in. square piles with 3 in. cover

It appears that most 14 in. (350 mm) piles using 3 in. (76.2 mm) of cover are for either state department of transportation related projects (not governed by the axial load limits of the 2018 IBC[7]) or marine projects with low axial loads. All pile configurations presented in Tables 1 through 10 (modified to include 3 in. of cover) result in *%Drop* greater than 60%. **Figure 11** presents the best results obtained for one of the circular configurations considered. All 14 in. piles with 3 in. of cover (both circular and square strand configurations) should continue to use an axial load limit of $0.20 f'_c A_g$, as no improved performance was noted by the research.

Conclusion

The primary goal of this research project was to closely examine the moment-curvature behavior of 14 in. (350 mm) prestressed concrete piles with axial loads greater than $0.2 f'_c A_g$. Previous research by Fanous et al.[9] opined that significant moment drops larger than 40% of the first peak moment could result in unreliable seismic performance and concluded that the most effective way of managing the desired limit on the drop in moment was to limit the axial load to $0.2 f'_c A_g$.

Assuming that the 40% drop is actually a concern, the results presented in this paper suggest that more accurate axial load limits can be established.

For circular spiral and strand configurations with 2 in. (76.2 mm) cover, use the following:

- $0.30 f'_c A_g$ when the effective prestress is 700 psi (4830 kPa)
- $0.25 f'_c A_g$ when the effective prestress is 1200 psi (8270 kPa)

Linear interpolation between $0.30 f'_c A_g$ and $0.25 f'_c A_g$ may be used for effective prestress values between 700 and 1200 psi (4830 and 8270 kPa), respectively.

Figure 12 shows the impact of adopting the suggested increase in the axial load limit. The moment-curvature behavior and stability remain almost completely unchanged. Although there is a slightly increased moment drop for the

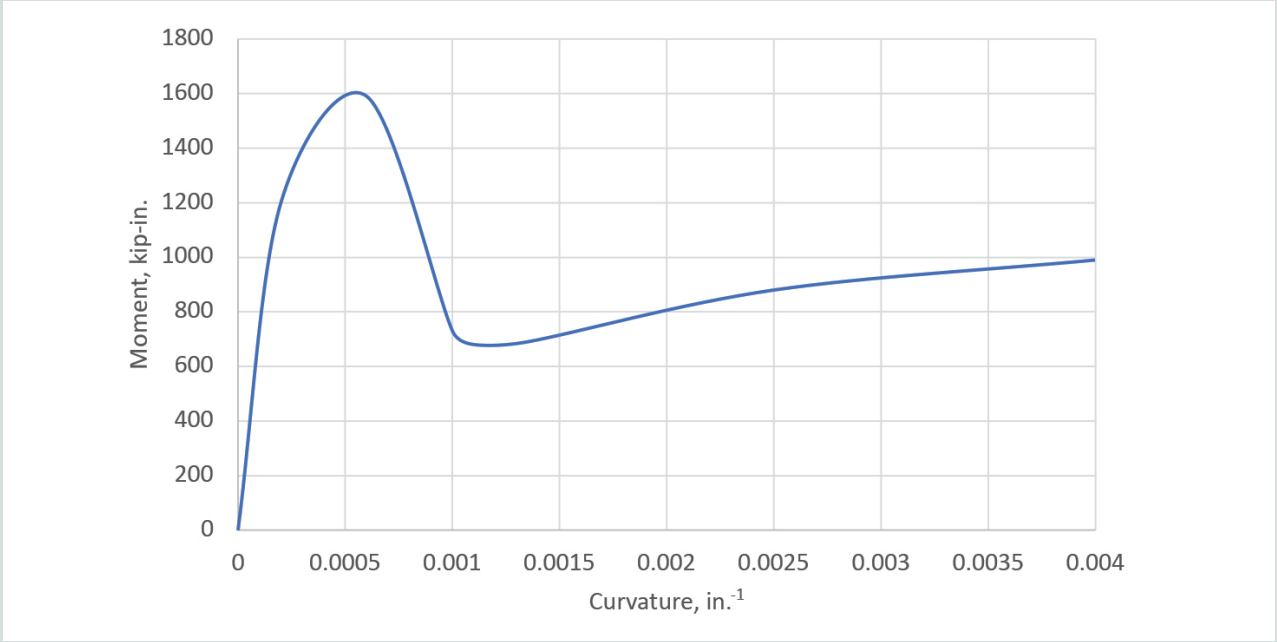

Figure 11. Best shape of full moment-curvature curve with 3 in. of cover. Note that *%Drop* = 43% and *%Return* = 63%. This case can be compared with the results of row 1 of Table 2, which are for 2 in. of cover. Note: M_{drop} = minimum moment that occurs after $M_{peak,1}$ on the moment-curvature curve; $M_{peak,1}$ = first maximum moment that occurs on the moment-curvature curve; $M_{peak,2}$ = second maximum moment that occurs after M_{drop} on the moment-curvature curve; *%Drop* = ratio $M_{drop}/M_{peak,1}$; *%Return* = ratio $M_{peak,2}/M_{peak,1}$. 1 in. = 25.4 mm; 1 kip-in. = 0.113 kN-m.

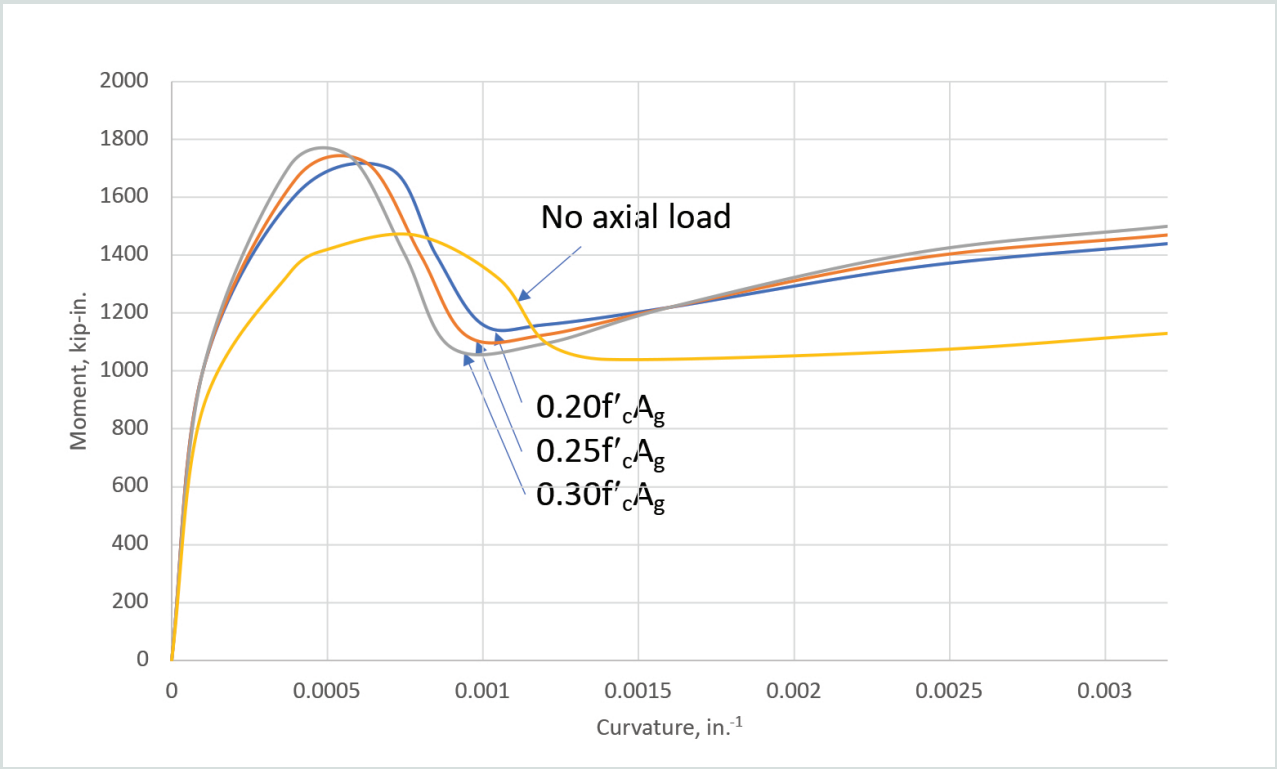

Figure 12. Typical curves showing increased moment drop as axial load is increased. Note: A_g = gross cross-sectional area; f'_c = specified 28-day strength of the concrete. 1 in. = 25.4 mm; 1 k-in. = 0.113 kN-m.

increased axial load, there is also an increase in the second maximum moment that occurs after M_{drop} on the moment-curvature curve $M_{peak,2}$. As such, the energy dissipated appears to be unrelated to the axial loads applied. Although the minimum axial load considered in this study is 0.20 $f'_c A_g$, the significant drop in moment occurs even with no axial load applied to the pile. In other words, the moment-curvature response for a pile with zero axial load is only nominally better than the same pile with an axial load ratio equal to 0.35 when coupling seismic performance to a drop in the moment. Therefore, the use of an axial load limit as a means of ensuring acceptable seismic performance may not be reasonably justifiable.

For square confinement and strand configurations with 2 in. (76.2 mm) cover: 0.35 $f'_c A_g$ when the effective prestress is between 700 and 1200 psi (4830 and 8270 kPa). Note that square confinement was not considered by Fanous et al.[9]

Based on the results of this research study, the research team recommends that the following options be considered:

- Eliminate the axial load limit for prestressed piles. It is the authors' opinion that the axial load limits for pile ductility applied to piles are unusual and already accounted for directly in vetted codes and standards used in the United States, not appropriate for prestressed piles because the moment strength returns in a reliable manner following the moment drop, and based on a performance requirement not mandated in the codes for other products, such as auger-cast and proprietary pile systems.

- If code committees desire an axial load limit to be maintained, the authors suggest that the axial load limits for 14 in. (350 mm) square piles be increased as justified by the findings of this paper. The authors' discussions with pile producers and designers of 14 in. piles in areas of high seismicity suggest that the increased limits established in this report would be in line with axial loads normally considered in design.

- Where 3 in. (76.2 mm) of cover is required, the authors recommend that the outer 1 in. (25.4 mm) of concrete be considered sacrificial and not included in the cross-sectional analysis calculations used to design the pile. The results of this paper can then be utilized but a significant reduction in moment capacity should be expected (that is, the pile will behave more like a 12 in. [305 mm] pile).

- Although auger-cast piles are outside the scope of this paper, Fig. 2 suggests that they can perform significantly worse than prestressed piles of the same size with respect to moment drop. In addition, the auger-cast pile response considered does not exhibit a second peak moment. This general response exhibited by auger-cast piles may tend toward the exact failure mechanism that limiting the moment drop seeks to address. At a minimum, if concrete design codes limit prestress pile axial loads due to percent drop in peak moment to prevent instability, other concrete foundation elements should conform to the same limitations.

Previous experimental research on the seismic design of prestressed piles has focused primarily on the ductility of pile hinges under cyclic loading. The condition of the exposed pile hinge after a major earthquake would also be important in regard to pile repair and potential future use without repair or replacement. Although analytical models used in this study and previous experimental research suggest that piles maintain their prestress after multiple reversed cyclic loads, the fact that many pile hinges would occur in areas that are not repairable makes this an important area of future research.

Acknowledgments

The authors wish to thank PCI for its support. The research discussed in this paper would not be possible without the financial support from PCI and the input from PCI committee members.

References

1. ICBO (International Conference of Building Officials). 1997. *Uniform Building Code*. Whittier, CA: ICBO.

2. ICC (International Code Council). 2015. *International Building Code*. Country Club Hills, IL: ICC.

3. Banerjee, S., J. F. Stanton, and N. M. Hawkins. 1987. "Seismic Performance of Precast Concrete Bridge Piles." *Journal of Structural Engineering* 113 (2): 381–396.

4. Budek, A. M., G. Benzoni, and M. J. N. Priestly. 1997. *Experimental Investigation of Ductility of In-Ground Hinges in Solid and Hollow Prestressed Piles*. Report SSRP-97/17, University of California San Diego.

5. Sritharan, S., A. Cox, J. Huang, M. Suleiman, and K. Arulmoli. 2016. "Minimum Confinement Reinforcement for Prestressed Concrete Piles and a Rational Seismic Design Framework." *PCI Journal* 61 (1): 51–69.

6. PCI Committee on Prestressed Concrete Piling. 2019. "Recommended Practice for Design, Manufacture, and Installation of Prestressed Concrete Piling." *PCI Journal* 64 (4): 84–116.

7. ICC. 2018. *International Building Code*. Country Club Hills, IL: ICC.

8. ACI (American Concrete Institute) Committee 318. 2019. *Building Code Requirements for Structural Concrete (ACI 318-19) and Commentary (ACI 318-19R)*. Farmington Hills, MI: ACI.

9. Fanous, A., S. Sritharan, M. Suleiman, J. Huang, and K. Arulmoli. 2010. "Minimum Spiral Reinforcement Requirements and Lateral Displacement Limits for Prestressed Concrete Piles in High Seismic Regions." Final report to PCI. ISU-ERI-Ames report ERIERI-10321, Department of Civil, Construction, and Environmental Engineering, Iowa State University, Ames, IA.

10. Michael N. Fardis, Eduardo C. Carvalho, Peter Fajfar, and Alain Pecker. 2015. *Seismic Design of Concrete Buildings to Eurocode 8*. Boca Raton, FL: CRC Press.

11. ASCE/SEI Committee 41. 2017. *Seismic Evaluation and Retrofit of Existing Buildings*. ASCE/SEI 41-17. Reston, VA: American Society of Civil Engineers.

12. California State Lands Commission. 2016. "Marine Oil Terminals." In Title 24, *California Code of Regulations*, Part 2, California Building Code. Long Beach, CA: California State Lands Commission.

13. ASCE/COPRI Committee 61. 2014. *Seismic Design of Piers and Wharfs*. ASCE/COPRI 61-14. Reston, VA: American Society of Civil Engineers.

14. Port of Long Beach. 2015. *Port of Long Beach Wharf Design Criteria*. Long Beach, CA: Port of Long Beach.

15. South Carolina Department of Transportation. 2008. *SCDOT Seismic Design Criteria*. Columbia, SC: South Carolina Department of Transportation.

16. ASTM A416. 2018. *Standard Specification for Low-Relaxation, Seven-Wire Steel Strand for Prestressed Concrete*. ASTM A416/A416M-18: West Conshohocken, PA: ASTM International.

17. ASTM Subcommittee A01.05. 2010. *Standard Specification for Steel Wire and Welded Wire Reinforcement, Plain and Deformed, for Concrete*. ASTM A1064/ A1064M-10. West Conshohocken, PA: ASTM International.

18. Mander, J. B., M. J. N. Priestley, and R. Park. 1988. "Theoretical Stress-Strain Behavior of Confined Concrete." *Journal of the Structural Division* 114 (8): 1804–1825.

19. Ryan, J. C., and T. W. Mays. 2020. *Axial Load Limit Considerations for 14 in. Prestressed Concrete Piles Reconciling the 2018 IBC and ACI 318-19 Prestressed Pile Axial Load Limits with PCI's 2019 Recommended Practice for Design, Manufacture, and Installation of Prestressed Concrete Piling*. Report no. CIT-CEE-1, The Citadel, Charleston, SC.

Notation

A_g = gross cross-sectional area

A_{sh} = total cross-sectional area of transverse reinforcement provided separately in each direction, including crossties where applicable

A_{sp} = cross-sectional area of spiral reinforcement

f_c = stress in concrete

f_c' = specified 28-day strength of the concrete

f_{cc}' = ultimate stress in confined concrete

f_{co}' = stress in unconfined concrete

f_{pc} = effective prestress in the pile

f_{pu} = ultimate strength of prestressing strand

f_{yh} = yield strength of spiral reinforcement

h_c = confined concrete side dimension defined by transverse steel dimension

M_{drop} = minimum moment that occurs after $M_{peak,1}$ on the moment-curvature curve

M_{max} = maximum moment

M_p = plastic or maximum moment on the bilinear idealized moment-curvature curve

$M_{peak,1}$ = first maximum moment that occurs on the moment-curvature curve

$M_{peak,2}$ = second maximum moment that occurs after M_{drop} on the moment-curvature curve

M_{sh} = moment at strain hardening

M_u = ultimate moment

P = axial load on the pile

$\%Drop$ = ratio of M_{drop} to $M_{peak,1}$

$\%Return$ = ratio of $M_{peak,2}$ to $M_{peak,1}$

s = longitudinal spacing of the transverse steel

Δ = pile deflection

ε_c = strain in concrete

ε_{cc} = strain in confined concrete at peak stress

ε_{co} = strain in unconfined concrete at peak stress

ε_{cu} = ultimate strain in concrete

ε_{spall} = strain at unconfined concrete spalling

θ_u = ultimate rotation of the plastic hinge

ρ_s = quantity of confinement spiral

ϕ_{cr} = curvature at the initiation of tension cracking

ϕ_m = maximum curvature

ϕ_{max} = maximum curvature

ϕ_p = plastic curvature

ϕ_{sh} = curvature at strain hardening

ϕ_{sp} = curvature associated with the initiation of unconfined concrete spalling

ϕ_u = ultimate curvature

About the authors

Timothy W. Mays, PhD, PE, is a professor of civil engineering at The Citadel in Charleston, S.C. He actively participates in PCI-related research and on standards development committees through PCI and the American Society of Civil Engineers. He obtained his doctorate in civil engineering from Virginia Polytechnic Institute and State University in Blacksburg, Va., in 2000. His areas of expertise are code applications, structural design, foundations, seismic design, steel connections, structural dynamics, coastal design, and civil engineering aspects of antiterrorism.

John C. Ryan, PhD, PE, is an assistant professor of civil engineering at The Citadel in Charleston, S.C. He provides structural foundation engineering services through Ryan Structural Engineers LLC. He is actively involved with prestress pile research through PCI. He obtained his doctorate in civil engineering from Virginia Polytechnic Institute and State University in Blacksburg, Va., in 2006.

Abstract

The 2018 *International Building Code* and *American Concrete Institute Building Code Requirements for Structural Concrete (ACI 318-19) and Commentary (ACI 318R-19)* have adopted axial load limits that prohibit the use of some 14 in. (350 mm) square prestressed concrete piles in areas of moderate to high seismicity. This paper presents the results of a study that examined the development of these axial load limits, their appropriateness as an attempt to ensure reliable seismic performance, and the expected seismic performance of commonly used 14 in. (350 mm) square prestressed concrete piles when the axial load limit is increased to levels commonly used in seismic design practice. Results of the study suggest that the axial load limits established by previous researchers are overly conservative and do not ensure reliable seismic performance. This paper recommends that reduced nominal moment strength be used in lieu of axial load limits for consistency with codified approaches already used in the United States and to help ensure reliable seismic performance when appropriate.

https://doi.org/10.15554/pcij66.6-02

Keywords

Axial load limit, confinement, design, foundation, pile, seismic.

Review policy

This paper was reviewed in accordance with the Precast/Prestressed Concrete Institute's peer-review process.

Reader comments

Please address any reader comments to *PCI Journal* editor-in-chief Tom Klemens at tklemens@pci.org or Precast/Prestressed Concrete Institute, c/o PCI Journal, 8770 W. Bryn Mawr Ave., Suite 1150, Chicago, IL 60631.